UICC

BINDING AND INTERSTITIAL PENETRATION OF LIPOSOMES WITHIN AVASCULAR TUMOR SPHEROIDS

Kostas Kostarelos[1], Dimitris Emfietzoglou[2], Alexandros Papakostas[2], Wei-Hong Yang[3], Åse Ballangrud[3] and George Sgouros[3]*

[1]*Imperial College Genetic Therapies Centre, South Kensington Campus, Imperial College London, United Kingdom*
[2]*Department of Medical Physics, School of Medicine, University of Ioannina, Ioannina, Greece*
[3]*Department of Medical Physics, Memorial Sloan-Kettering Cancer Institute, New York, NY, USA*

The liposomal delivery of cancer therapeutics, including gene therapy vectors, is an area of intense study. Poor penetration of liposomes into interstitial tumor spaces remains a problem, however. In this work, the penetration of different liposomal formulations into prostate carcinoma spheroids was examined. Spheroid penetration was assessed by confocal microscopy of fluorescently labeled liposomes. The impact of liposomal surface charge, mean diameter, lipid bilayer fluidity and fusogenicity on spheroid penetration was examined. A variety of different liposome systems relevant to clinical or preclinical protocols have been studied, including classical zwitterionic (DMPC:chol) and sterically stabilized liposomes (DMPC:chol:DOPE-PEG$_{2000}$), both used clinically, and cationic liposomes (DMPC:DOPE:DC-chol and DOTAP), forming the basis of the vast majority of nonviral gene transfer vectors tested in various cancer trials. Surface interactions between strongly cationic vesicles and the tumor cells led to an electrostatically derived binding-site barrier effect, inhibiting further association of the delivery systems with the tumor spheroids (DMPC:DC-chol). However, inclusion of the fusogenic lipid DOPE and use of a cationic lipid of lower surface charge density (DOTAP instead of DC-chol) led to improvements in the observed intratumoral distribution characteristics. Sterically stabilized liposomes did not interact with the tumor spheroids, whereas small unilamellar classical liposomes exhibit extensive distribution deeper into the tumor volume. Engineering liposomal delivery systems with a relatively low charge molar ratio and enhanced fusogenicity, or electrostatically neutral liposomes with fluid bilayers, offered enhanced intratumoral penetration. This study shows that a delicate balance exists between the strong affinity of delivery systems for the tumor cells and the efficient penetration and distribution within the tumor mass, similar to previous work studying targeted delivery by ligand-receptor interactions of monoclonal antibodies. Structure-function relationships from the interaction of different liposome systems with 3-dimensional tumor spheroids can lead to construction of delivery systems able to target efficiently and penetrate deeper within the tumor interstitium and act as a screening tool for a variety of therapeutics against cancer.
© *2004 Wiley-Liss, Inc.*

Targeted tumor delivery of therapeutic agents using liposomes has so far led to the design of a wide variety of systems, primarily enhancing the tumor-to-blood concentration of the carrier-drug complex at the target site. Tumor targeting of liposomes can be achieved either by active or passive targeting.[1] Some of the moieties attached onto the liposome surfaces to achieve cell receptor-specific (active) targeting include antibodies,[2,3] antibody fragments,[4,5] vitamins,[6] proteins,[7,8] oligopeptides[9,10] and oligosaccharides,[11] while nonspecific (passive) targeting mainly by leakage through solid tumor vasculature has been achieved by attaching ganglioside (GM$_1$)[12,13] and polymer molecules.[14–16]

Despite the effective pharmacologic profiles obtained for a variety of targeted liposome-encapsulated therapeutics,[17] one of the most important obstacles in achieving highly effective liposomal delivery, particularly in the case of solid tumor therapy, is their limited intratumoral transport. The poor ability of liposomes to diffuse within the interstitial space of the tumor and carry their load to cells distant from the vascular bed and as close to the hypoxic and necrotic regions as possible dramatically restricts the overall therapeutic effect achieved, leading to undesirable relapse. Even in the case of sterically stabilized liposomes, which are able to extravasate adequately from the leaky tumor microcapillaries, it has been reported that following extravasation, liposomes and their drug loads reside in areas very proximal to the vasculature, resulting in inhomogeneous and ultimately inefficient delivery of the cytotoxic drugs carried.[18–21] Any improvement in the ability of liposomes to deliver their loads deeper within the tumors will help diminish tumor regrowth events post-therapeutically and maximize the overall therapeutic index achieved.

Spheroids are 3-dimensional (spherical) clusters of tumor cells grown from one or several cell clones.[22,23] Spheroids contain many of the elements of a tumor xenograft, including an extracellular matrix (ECM) and cell-cell/cell-matrix interactions;[24] a spatial geometry that can produce well-defined nutrient concentration;[25,26] and subpopulations of cells that are quiescent, hypoxic and necrotic.[27] These similarities to a tumor xenograft are coupled with many of the experimental advantages of a cell culture, including the ability to monitor and control experimental and treatment conditions rigorously, as well as study the mechanisms of cellular response to therapeutic (or other) agents. Moreover, tumor sphe-

Dr. Kostarelos's current address is: Centre for Drug Delivery Research, The School of Pharmacy, 29-39 Brunswick Square, University of London, WC1N 1AX London, U.K. E-mail: kostas.kostarelos@ulsop.ac.uk

*Correspondence to: Division of Nuclear Medicine, Department of Radiology, Johns Hopkins School of Medicine, 220 Ross, 720 Rutland Avenue, Baltimore, MD 21205. Fax: +413-487-3753.
E-mail: gsgouros@jhmi.edu

roids are continuously being utilized as models for the study of early tumor development,[28,29] models of avascular micrometastastatic tumors[30–32] and, particularly in scope of the present study, as models of the tumor interstitial space (despite the absence of vasculature and endogenous humoral agents).[33,34]

In this work, the multicellular tumor spheroid model has been utilized to study passive (nonspecific) targeting through electrostatic surface binding and interstitial penetration and diffusion of a variety of liposome systems. Passive targeting of tumor vasculature by electrostatic binding has recently been studied *in vivo* using cationic liposomes alone[35] or in combination with targeting ligands.[9] In the present study, different types of fluorescently labeled liposomes were constructed and allowed to interact with tumor spheroids under controlled conditions; 200 μm diameter spheroids were chosen as these are at the edge of exhibiting hypoxic and necrotic cores,[36] the presence of which would be expected to complicate characterization of liposome penetration due to the accumulation of fluid and cellular debris. Using a quantitative evaluation based on confocal laser scanning microscopy and image analysis, the affinity for binding (nonspecific, passive targeting) and penetration (intratumoral diffusion) exhibited by the different liposome systems was studied.

MATERIAL AND METHODS

Lipids and liposomes

Different types of liposomes, representing liposomes commonly used for biomedical applications (delivery of anthracyclines, amphotericin, plasmid DNA) were allowed to interact with tumor spheroids. All liposome compositions were prepared as multilamellar vesicles (MLVs) and small unilamellar vesicles (SUVs), differing in the mean particle size of the respective liposome populations. Light and electron microscopy indicated that the mean vesicle diameter for all MLV systems ranged between 800 and 1,000 nm, and for all SUV systems between 50 and 150 nm (not shown). The total lipid composition in the liposome systems was kept constant at 1 mg/ml throughout the study. All liposome systems were fluorescently labeled using a constant concentration (3.75 μg/0.5 mg lipid) of the lipophilic carbocyanine dye 1,1′-dioctadecyl-3,3,3′,3′-tetramethylindocarbocyanine perchlorate (DiI), which was previously shown to act as an efficient liposome bilayer marker for *in vivo* intraorgan localization studies.[37] Previous studies have shown that interaction between the lipid components of the liposomes and biologic molecules (such as serum lipoproteins contained in the cell culture medium) may occur without leading to significant deviations in the fluorescence signal intensity or its colocalization with the lipid vesicles.[38] Indeed, it has been shown that confocal microscopy fluorescence signal is colocalized with the liposome structures visualized by electron microscopy in different organs *in vivo*.[39]

DMPC, DC-chol, DPPC and cholesterol were purchased by Sigma-Aldrich (Poole, U.K.), DOTAP and DOPE-PEG$_{2000}$ were purchased by Avanti Polar Lipids (Alabaster, AL). All liposomes were prepared following the solvent evaporation-hydration protocol by solubilization of all lipids into laboratory-grade chloroform (USP) and subsequent evaporation under high pressure to form a lipid film. Hydration of the lipid films by addition of either PBS (in experiments not involving cells) or RPMI medium (for cellular experiments) produced multilamellar vesicles (MLVs). Extrusion cycles (10) through polycarbonate filters (Millipore, Bedford, MA) using a LiposoFast extruder (Avestin, Ottawa, Canada) was used to form small unilamellar liposomes according to a previously described protocol.[40]

Liposome surface characterization

The surface properties of the liposomes were characterized using a DELSA 440 Zetasizer instrument by Beckman-Coulter (Fullerton, CA). Ten different measurements for each liposome system were carried out and all 4 different angles of detection were used to obtain the ζ potential at the liposome surface by employing the Smoluchowski approximation on the electrophoretic mobility

data obtained when a 5 V electric field was applied to the liposome suspension: $U = \epsilon\zeta / \eta$, where U is electrophoretic mobility, ϵ is permittivity of the medium ($\epsilon = \epsilon_o D$, where ϵ_o is permittivity of free space and D is dielectric constant), η is viscosity and ζ is zeta potential.

Cells and spheroids

Multicellular spheroids consisting of the LNCap-LN3 prostate tumor cell line were prepared according to the liquid overlay technique of Yuhas *et al.*[41] as described in detail previously.[36] Approximately 10^6 LNCaP-LN3 cells, obtained by trypsinization from growing monolayer cultures, were seeded into 100 mm dishes coated with a thin layer of 1% agar (Bacto Agar; Difco, Detroit, MI) with 15 ml of RPMI-1640, supplemented with 10% fetal bovine serum, 100 units/ml penicillin and 100 μg/ml streptomycin. After 3–5 days in the agar culture, spheroids of 200 ± 20 μm in diameter were selected under an inverted phase-contrast microscope with an ocular scale using an Eppendorf pipette. The selected spheroids were transferred to 35 mm bacteriologic Petri dishes in 2 ml of medium.

Interaction between liposomes with spheroids

Multicellular spheroids were coincubated with liposomes in 35 mm diameter Petri dishes for 2, 5 and 24 hr at 37°C. All incubations were undertaken in an orbital shaker incubator. At the specified time points, spheroids were washed 3 times with PBS and placed in fresh incubation medium before fluorescence imaging was carried out; selected spheroids were not washed prior to imaging. Five spheroids were studied in each condition.

Confocal laser scanning fluorescence microscopy

CLSM imaging (Zeiss LSM 510; Carl Zeiss, Oberkochen, Germany) was carried out by acquiring 3 μm thick optical sections of the spheroids under study from the top toward the center of the spheroids until approximately scanning 120 μm deep into the spheroid. DiI fluorescence was observed red using standard rhodamine optics (excitation filter at 546 nm, dichroic mirror at 580 nm and barrier filter at 590 nm), as previously described.[38]

Image analysis

The fluorescence profile of each spheroid as a function of depth was determined from the average intensity along 50 equally spaced spheroid diameters using the image analysis software Intelligent View (version 1.2 by Bokwon Yoon). For each spheroid image, the obtained radial profiles were corrected for background fluorescence based on the light intensity around the spheroid, as well as for the exponential light attenuation due to scattering and absorption within the spheroid. The linear attenuation coefficient was determined in separate experiments from spheroids of autofluorescent cells transfected with a fluorescent protein.[32] Attenuation was modeled by the expression $I = I_0 \exp(-ar)$, where r is a variable representing the perpendicular distance between the focal plane imaged and the proximal surface of the spheroid, a is the attenuation coefficient and I_0 is the fluorescent intensity at the rim of the spheroid (in which attenuation is assumed negligible). Using this expression, the attenuation coefficient, a, was found to be 0.003165/μm. Quantitative fluorescence intensity data are from spheroids from at least 2 separate experiments. Five spheroids were included per condition per experiment. The fluorescence data collected were then analyzed to yield the following parameters: binding, taken as the percentage of total fluorescence intensity found in a 20 μm shell surrounding the spheroid rim ($\sim$ 2–3 cell layers); affinity, taken as the total fluorescence intensity signal from each image. The percentage of fluorescence intensity (relative to peak intensity) found at 50 and 100 μm radial distance from the outer spheroid periphery is used to obtain a 2-component description of diffusion or penetrative capacity (*i.e.*, penetration at equilibrium state) for each liposome system examined.

It is important to note that the CM-based methodology used to evaluate vesicle penetration into spheroids is an alternative to the

autoradiography procedures typically used to obtain quantitative information regarding drug and vesicle penetration. Although the CM approach is not as inherently quantitative as autoradiography, the methodology offers the advantages of being a radiation-free technique in which tomographic distribution information may be obtained rapidly in living cell samples without the requirement for sectioning and week- to month-long exposure times.

RESULTS

Various types of liposome systems were constructed and allowed to interact with the tumor spheroids. The liposome systems prepared and their surface charge (ζ potential) data from the laser electrophoresis experiments are depicted in Table I. The variation in liposome surface and lipid bilayer characteristics and the ensuing ability to interact with cellular membranes should be noted. In Figure 1, the confocal laser scanning microscopy (CLSM) and differential interference contrast images of the equatorial slice images of LNCaP-LN3 spheroids following interaction with fluorescently labeled SUVs formed with DMPC:chol (Fig. 1*a*), DMPC:DC-chol (Fig. 1*b*), DPPC:chol (Fig. 1*c*) and DMPC:chol:DOPE-PEG$_{2000}$ (Fig. 1*d*) are shown. Apart from the notable association and intraspheroid diffusion exhibited by the DMPC:chol SUVs (Fig. 1*a*), what is also striking is the limited interaction of the cationic DMPC:DC-chol SUVs (Fig. 1*b*) at the very edge of the outer spheroid rim. DPPC:chol liposomes (Fig. 1*c*) indicated that hardly any interaction was taking place between them and the spheroid. Similarly, in the case of sterically stabilized DMPC:chol:DOPE-PEG$_{2000}$ (Fig. 1*d*), even though present in the vicinity of the spheroid, the polymer layer at their surface seems to exclude any binding or penetration within the spheroid. The fluorescence signals in the environment surrounding the spheroid in Figure 1(*d*) are apparent as no washing of this spheroid preceded the microscopic study.

A quantitative comparative analysis of the fluorescence intensity data obtained from the spheroid images depicts the dramatically different pattern of interaction occurring with the DMPC:chol and DMPC:DC-chol SUVs (Fig. 2). The latter, a strongly cationic liposome system, primarily binds to the outer cells at the spheroid surface, exhibiting a sharp decline in fluorescence intensity to almost zero values at approximately 30 μm within the spheroid. Contrary to that, the DMPC:chol liposomes not only associate with the tumor spheroids, but also penetrate extensively almost throughout the interstitial space. Figure 3 shows that only a moderate improvement in the penetrative capacity of DMPC:chol SUVs was obtained, when allowing interaction with the spheroids for 2 and 5 hr. This is more clearly illustrated in the analysis of fluorescence profiles (Fig. 3*c*); a 40–50% increase in the fluorescence intensity toward the spheroid center is observed between 2 and 5 hr.

To elaborate on the construction and properties of the liposome systems, we engineered several different positively charged (cationic) vesicles containing the fusogenic lipid DOPE.[42] In Figure 4, equatorial slice images of spheroids following interaction with multilamellar vesicles for 2 and 5 hr are shown. The cationic MLVs of DMPC:DC-chol adhere to the surface of the spheroid (Fig. 4*a*) and after 5 hr only a moderate increase in the accumulation of vesicles at the spheroid surface was observed (Fig. 4*b*). Addition of the fusogenic lipid DOPE in the vesicle content led to an improvement in the vesicle interaction with the outer tumor cells; however, no dramatic augmentation of penetration of the spheroids was obtained (Fig. 4*c*). After 5 hr, more DMPC:DC-chol:DOPE MLVs were binding strongly onto the spheroid, but without any appreciable intratumoral diffusion occurring (Fig. 4*d*). Altering the cationic lipid used to DOTAP, MLVs of DMPC:DOPE:DOTAP exhibited a dramatic increase in both the amount of vesicles binding and fusing with the spheroids (Fig. 4*e*). Moreover, allowing the vesicles to interact with the spheroid for 5 hr seemed to improve the extent of fusion taking place with the tumor cells (Fig. 4*f*). In Figure 5, the quantitative depiction of fluorescence intensity for a series of images using the liposome systems shown in Figure 4 is represented. Overall, DOPE inclusion in the lipid bilayers offered a homogeneous interaction with the spheroids, improving both electrostatic targeting and diffusion within the spheroid by 20% compared to lipid bilayer liposomes that did not contain any DOPE (Fig. 5). A further, almost 2-fold improvement in both affinity for the spheroid surface and diffusion within the model tumor tissue was obtained by using the cationic lipid DOTAP instead of DC-cholesterol.

Small unilamellar vesicles of the 3 cationic systems were allowed to interact with the tumor spheroids for 2 hr. Representative CLSM equatorial images of the spheroids are shown in Figure 6. The DMPC:DC-chol and DMPC:DOPE:DC-chol SUVs (Fig. 6*a* and *b*) displayed binding limited to the surface of the spheroid. The addition of the fusogenic DOPE led to an evident increase in the amount of fluorescence intensity at the spheroid rim, particularly evident in the quantitative results of Figure 7. DOPE inclusion, however, only led to a 2-fold increase of fluorescence intensity signal obtained at the outer cell layers of the spheroid, without any evident improvement in the intratumoral diffusion of liposomes. Interestingly, DOPE in the MLV systems had a pronounced effect in both total affinity and diffusion. The DMPC:DOPE:DOTAP SUV system exhibited the most homogeneous distribution throughout the tumor spheroid and also an evident fusogenic capability. In Figure 6(*c*), in a representative CLSM image of a spheroid interacting with the DMPC:DOPE:DOTAP system, individual cells deep within the spheroidal cluster are fluorescently tagged by the liposomes. From the data obtained quantitatively and depicted in Figure 7, the penetrative capabilities of the DMPC:DOPE:DOTAP SUV system can be observed with fluorescence intensities up to 100 μm toward the core of the spheroid, almost at the core of the tumor mass.

In Table II, the fluorescence signal intensity profiles of liposome-spheroid interactions have been analyzed to provide indications of the overall affinity for the tumor spheroid, as well as other intratumoral distribution characteristics (*i.e.*, binding and diffusion). It can be observed that all cationic liposomes exhibited strong overall affinity for the tumor spheroid. The extent of diffu-

TABLE I – LIPOSOME SYSTEMS STUDIED AND THEIR SURFACE CHARGE CHARACTERISTICS FROM ZETA POTENTIAL MEASUREMENTS CARRIED OUT USING LASER SCATTERING MICROELECTROPHORESIS AND THE LIPID BILAYER CHARACTERISTICS (AS DETERMINED BY THE RECORDED,[64] PHASE TRANSITION TEMPERATURES) OF THE SELECTED LIPID MOLECULES AT 37°C.

Liposome systems	Surface charge (mV)	Liposome bilayer characteristics (at 37°C)
DMPC:chol (2:1)	−9.3 ± 2.2	Liquid crystalline
DMPC:DC-chol (2:1)	51.7 ± 3.9	Liquid crystalline
DPPC:chol (2:1)	−55 ± 3.2	Gel
DMPC:chol:DOPE-PEG$_{2000}$ (10:5:1)	4.8 ± 0.4	Liquid crystalline
DMPC:DOPE:DC-chol (2:1:0.5)	55 ± 6.7	Fusogenic[1]
DMPC:DOPE:DOTAP (2:1:0.5)	49 ± 5.0	Fusogenic[1]

[1]The difference between those liposome systems is the charge:molecular weight ratio, which is 1:504 and 1:732 for the DC-chol and DOTAP, respectively.
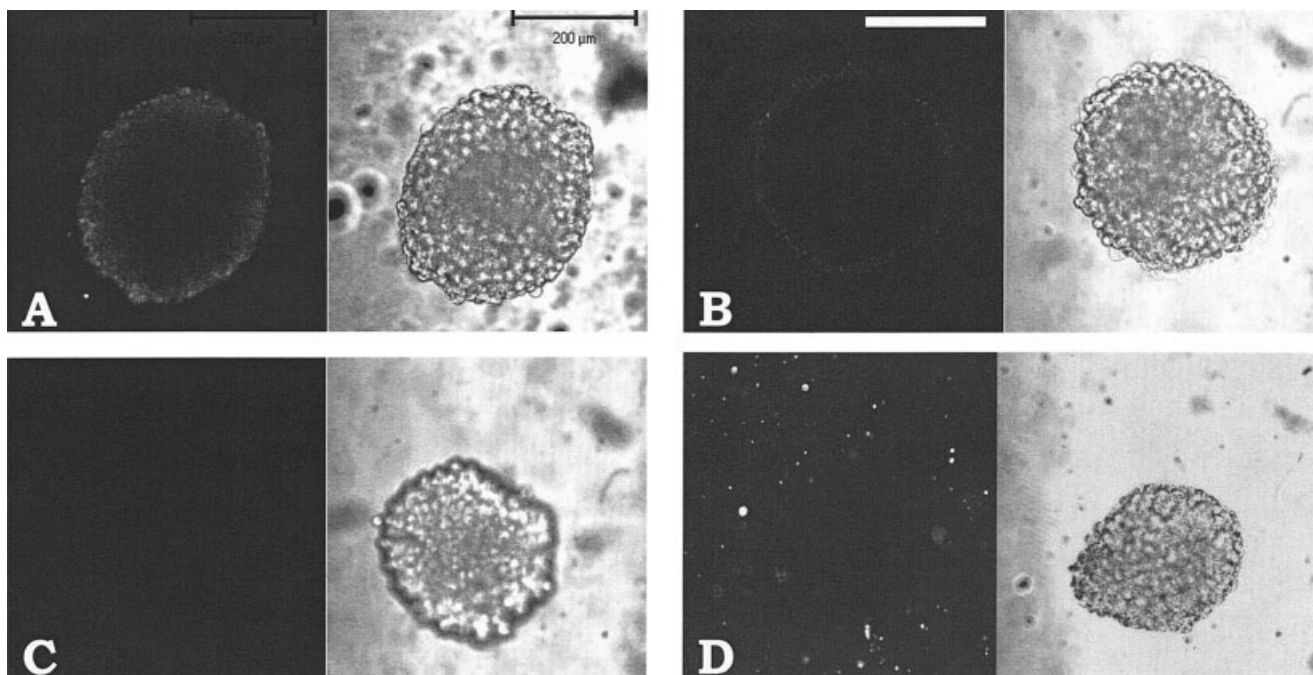
FIGURE 1 – The effect of different liposome types. CLSM images of spheroids (fluorescent and differential interference contrast images of the same field in each case) following interaction with small unilamellar vesicles composed of (*a*) DMPC:chol (washed); (*b*) DMPC:DC-chol (washed); (*c*) DPPC:chol (washed); (*d*) DMPC:chol:DOPE-PEG (unwashed). Spheroids and liposomes in all shown systems were coincubated for 2 hr at 37°C.
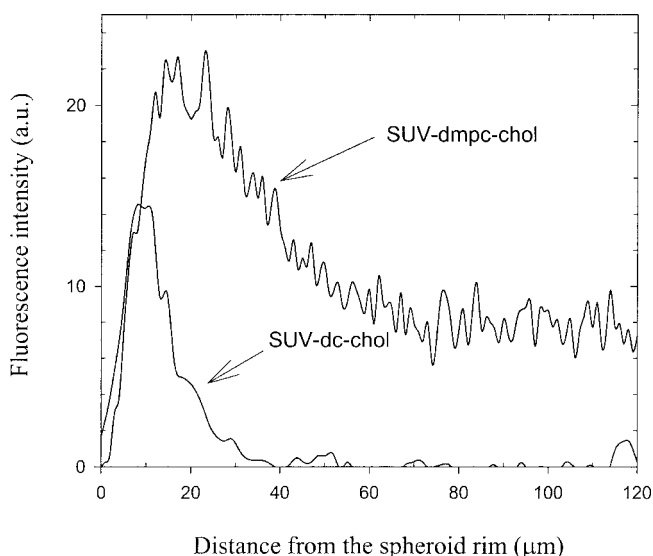

FIGURE 2 – The effect of liposome surface charge. Comparative fluorescence intensity (arbitrary units) profiles relative to distance from the spheroid rim to the center (0 μm is the edge of the spheroid rim) for the DMPC:chol and DMPC:DC-chol SUVs.

sion within the tumor volume was enhanced for the DMPC:chol SUV and the DMPC:DOPE:DOTAP SUV.

DISCUSSION

We have investigated the binding, permeability and diffusive distribution of liposome systems of various characteristics into multicellular spheroids used as *in vitro* models of avascular tumor bodies. Previously reported work, relevant to this study, involved the evaluation of the antiproliferative effects that free or liposome-encapsulated retinoic acid had on squamous carcinoma monolayers and spheroids,[43,44] and free or liposome-TNF-α on glioma (A172) multicellular spheroids.[45] Both of these studies reported effective delivery of the therapeutic molecules using liposomes compared to free drug, but did not investigate or attempt to correlate liposome characteristics with the interaction patterns and delivery into the tumor spheroid body. More recently, a study compared the improvement in doxorubicin diffusion within tumor spheroids between the free drug and the encapsulated drug in micelles and liposomes.[46] Strategies like that to improve the homogeneous distribution of drugs in tumor volumes by appropriately designed delivery systems can help overcome the barriers posed by the tumor physiology (such as interstitial pressure and pH and pO_2 levels).[47]

From the different types of liposomes tested here, only the ones with neutral and positive surface charge were able passively to target and diffuse within the spheroids in an efficient way. Sterically stabilized liposomes were not able to interact with the tumor cell cluster due to the PEG polymer coat on their surface (Fig. 1*d*) acting as a repulsive barrier against any attractive force with the cell surface. This result suggests that liposome vesicles surface-coated with large groups (polymeric, sugar, or other) essential to attain long-circulating properties will exhibit a pronounced limitation to travel intratumorally after extravasation from the tumor microcapillaries. This incapability of intratumoral transport has indeed been suggested previously in studies looking at the localization of stealth liposomes within the tumors *in vivo*.[18–21] Such observations, in combination with our findings, suggest that improvement of the therapeutic index of drugs (*e.g.*, liposome-encapsulated anthracyclines) can be achieved by delivery systems that once at the tumor interstitium lose their steric or stealth components, *e.g.*, by detachment or stimulated cleavage,[48] become able actively to transport or diffuse more efficiently within the tumor.
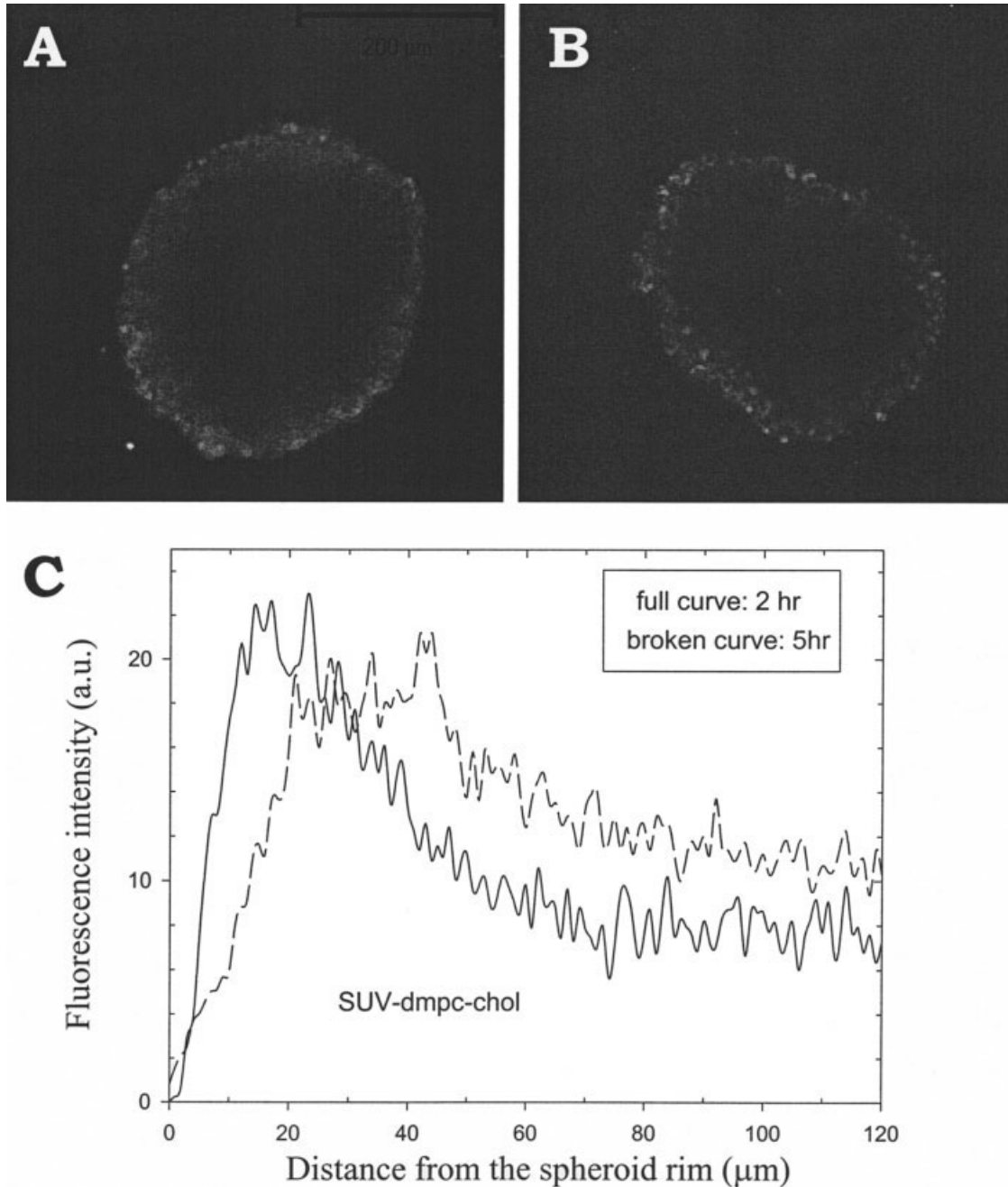
FIGURE 3 – The effect of duration of interaction. CLSM images of DMPC:chol (*a*) 2 and (*b*) 5 hr. (*c*) Their comparative fluorescence intensity profiles from the spheroid rim to the center.

Contrary to the well-documented time-dependent interaction between monoclonal antibodies and tumor spheroids toward developing actively targeted modalities against tumors,[32,49–51] liposomes seemed to reach an end state of interaction following rapid kinetics within the first 2 hr. Moreover, after 5 hr of interaction, minimal changes in both diffusion and binding were found throughout this study. However, as in the case of antibodies, the time necessary for maximum uptake of liposomes, or other delivery systems, within a tumor mass *in vivo* will normally be longer than within multicellular spheroids due to the different composition of the extracellular matrix and the interstitial fluid pressure, both reported to act as barriers to the delivery of therapeutic agents.[52] Such differences in the kinetic constants between actively or passively targeted carriers and spheroids or *in vivo* tumor

xenografts highlight the caution in extrapolating clinically relevant information from such studies.

Another apparent finding from this study is the pronounced ability of all cationic liposomes to interact with the spheroids (Figs. 4–7). MLV cationic liposomes exhibited enhanced binding for the multicellular spheroids, strongly binding and aggregating on the cellular surfaces. Cationic MLV systems despite their heavy binding, as expected from their large size dimension (0.8–1 μm in mean diameter, measured by quasielastic light scattering; not shown), lacked the ability to diffuse through the interstitial space of the spheroid, limiting their intratumoral penetration to the outer cell layers. Substantial (at least by a factor of 2) improvement in the diffusive capabilities of cationic liposomes was obtained when
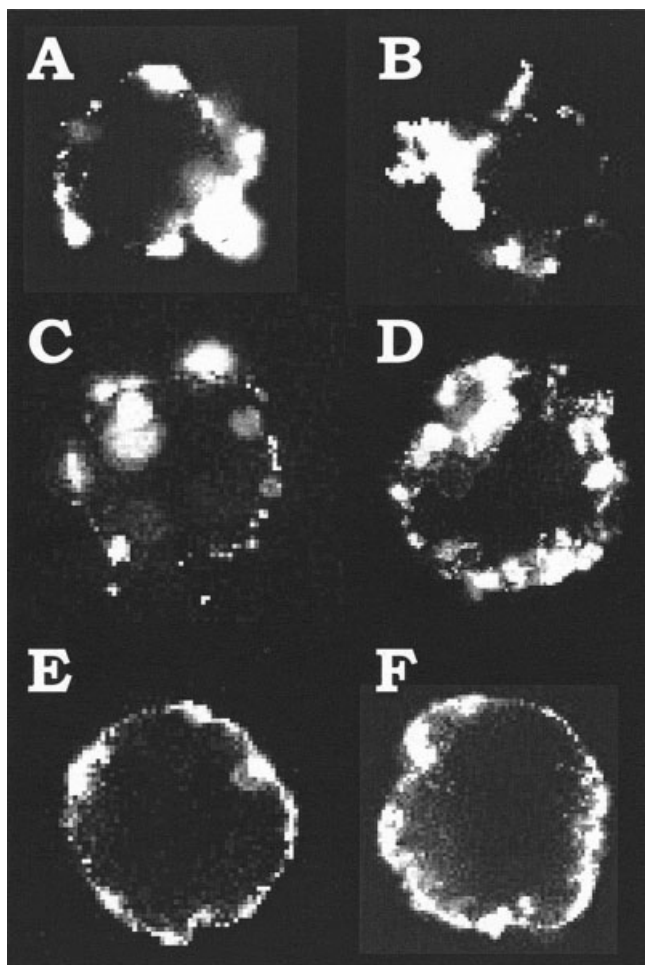
FIGURE 4 – Cationic surface and fusogenic bilayer character in multilamellar liposomes. CLSM equatorial slice (100 ± 10 μm) images of spheroids allowed to interact with MLVs of DMPC:DC-chol for (*a*) 2 and (*b*) 5 hr; DMPC:DOPE:DC-chol for (*c*) 2 and (*d*) 5 hr; DMPC:DOPE:DOTAP for (*e*) 2 and (*f*) 5 hr.
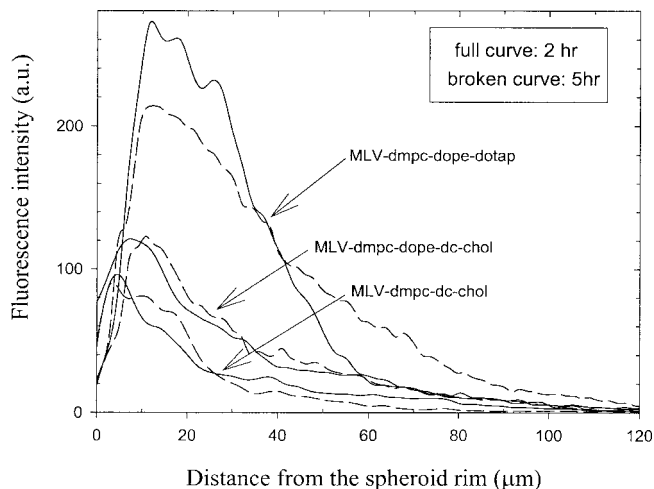

FIGURE 5 – Comparative fluorescence intensity (arbitrary units) profiles from the outer spheroid rim toward its center following interaction with the MLV systems depicted in Figure 4.

lipid bilayers were engineered to include the fusogenic DOPE lipid. Moreover, the retention and diffusion of cationic liposomes within the spheroids also depended on the molecular characteristics of the cationic lipid used to engineer the delivery vehicles. Optimization of the interaction was obtained when the cationic lipid DOTAP with a charge:molecular weight (1:732) ratio was used, instead of the cationic lipid DC-chol (1:504) with a higher molecular charge density. Inclusion of DOTAP improved the overall affinity for the spheroids by a factor of 2 (*i.e.*, 100%) compared to the DC-chol containing lipid bilayers, and the diffusion by almost a factor of 10 (Fig. 7), delivering fluorescence up to the spheroid core. The cationic liposomes containing DOTAP and the neutrally charged fusogenic DOPE lipid proved the most effective of all cationic vesicles formed and studied, both in terms of the targeting (binding) and diffusion (penetration) within the tumor spheroids.

Cationic liposomes have systematically been studied only in the last 15 years, principally due to their universal affinity for cell surfaces, an outcome of the electrostatic attractive force between their surface and the plasma membrane.[53] Their biologic and medical significance is getting established, as more types of cationic liposomes are engineered to deliver genetic material (DNA, RNA, oligonucleotides, artificial chromosomes) intracellularly. In fact, the most popular commercial transfection agents and the majority of the nonviral gene therapy vectors in clinical trials

today include DC-chol, DOPE, DOTAP, or their mixtures. Even though highly surface-charged cationic liposomes exhibit much shorter blood circulation half-lives than other more pharmacokinetically robust liposome systems when administered intravenously, there are clinical protocols being developed for their use in tumor treatments. Particularly in terms of targeted cancer therapeutics, cationic liposomes have been shown to be internalized specifically by tumor endothelial cells[35,54] and efficiently target the tumor neovasculature compared to anionic and neutral liposomes,[55] rendering them attractive delivery systems for antiangiogenic agents. In view of such applications, the present study suggests that use of cationic lipids with high molecular charge density to form liposomes can lead to strong binding with the cellular membranes. However, when delivery within more complex 3-dimensional structures (such as tumors or other tissues) is required, cationic liposomes should be engineered using molecules of lower charge density and enhanced fusogenic characteristics.

An important parameter of the interaction between tumor cell clusters and delivery vehicles is the extent of the binding-site barrier effect, detrimental to effective distribution within the tumor volume.[56,57] The binding-site barrier effect has been reported to become an increasingly significant factor in active (specific) targeting of tumors using monoclonal antibodies (MoAbs), particularly as the affinity of the targeting moieties for the cellular receptors increases as the number of receptors increases.[58,59] The importance of such an effect in the case of cationic liposomes interacting with the tumor spheroids has become evident in this study, as the strong electrostatic force between the vesicle and the cell surface saturates and congests the outer cell layers of the tumor cluster with aggregating liposomes (Figs. 4 and 5). In the systems that this effect was evident (namely, all DC-chol containing cationic liposomes), limited intratumoral distribution characteristics were observed. Passive targeting strategies, therefore, may be particularly susceptible to any physical (*e.g.*, electrostatic) binding-site barrier effects, as they utilize universal nonspecific interactions that may easily lead to unselective uneven distribution of the therapeutic agent within the target tissue.

The analysis presented in Table II illustrates the following points. One, positive charge at the liposome surface offered markedly effective binding and overall affinity for the spheroids, irrespective of mean particle size. Thus, in situations where labeling or tagging of tumor spheroids with a marker molecule (fluorescent or other) may be desirable, cationic liposomes can indeed act as effective marking tools. Two, adequate diffusion and penetration deep within the tumor spheroids, which will result in more homo-
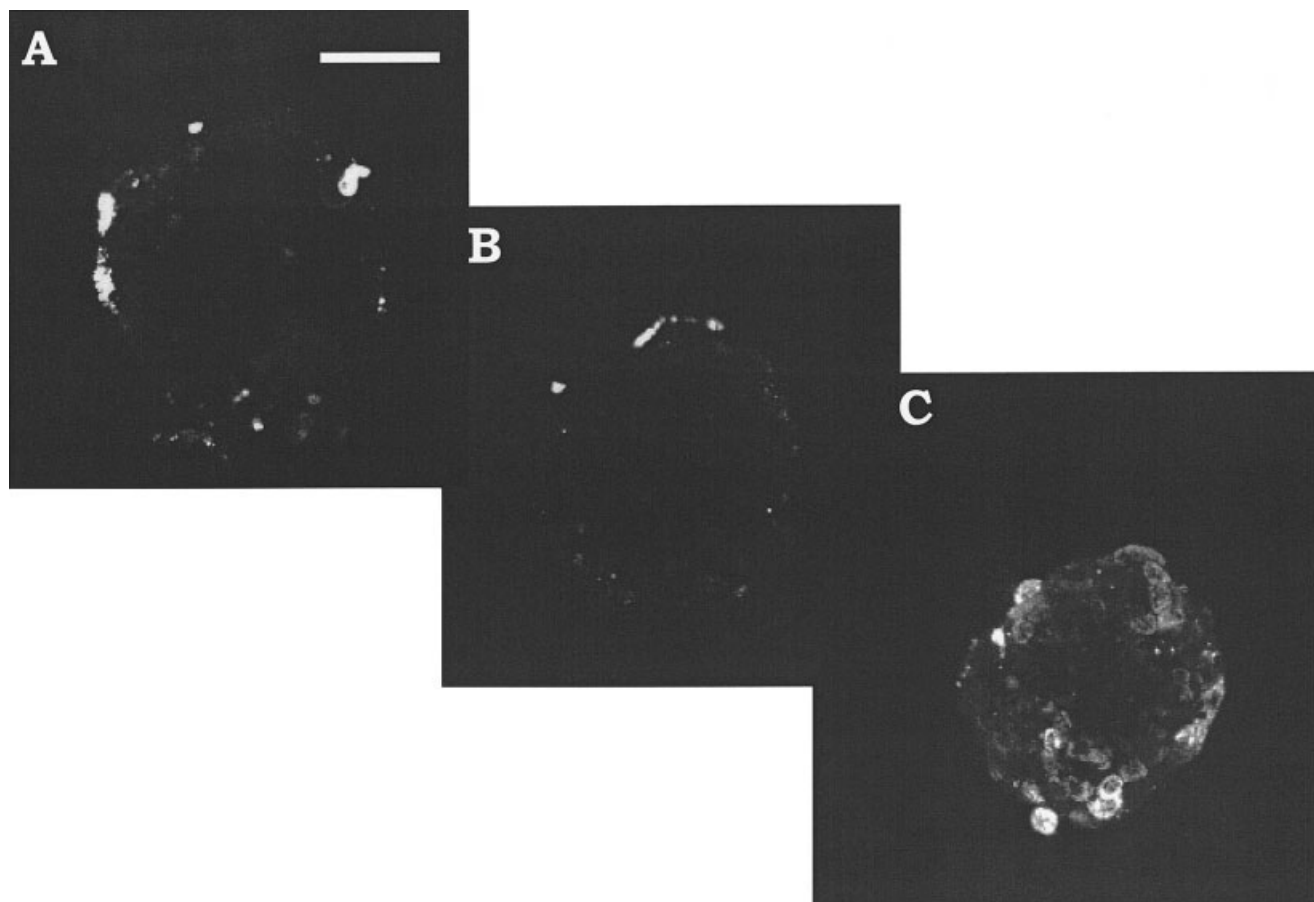
FIGURE 6 – Cationic surface and fusogenic bilayer character in small unilamellar liposomes. CLSM equatorial slice ($100 \pm 10 \mu m$) images of tumor spheroids following 2-hr interaction with SUVs containing (a) DMPC:DC-chol, (b) DMPC:DOPE:DC-chol and (c) DMPC:DOPE:DOTAP.
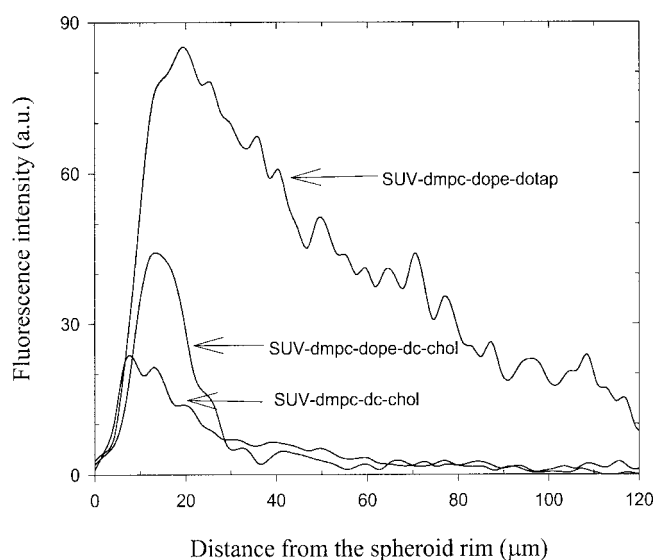

FIGURE 7 – Comparative fluorescence intensity (arbitrary units) profiles from the spheroid rim toward its center for the SUVs systems depicted in Figure 6.

geneous distribution throughout the avascular cell mass, is a much more intricate process requiring small particle size and a balance between liposome surface charge and bilayer fluidity. It is inter-

esting to note that only 2 SUV types of different surface and bilayer properties (neutral–DMPC:chol- and cationic/fusogenic-DMPC:DOPE:DOTAP) yielded notable fluorescence toward the spheroid core. This is particularly relevant to the efficacy of liposome-encapsulated drugs and suggests one possible mechanism for the low therapeutic indices that have been achieved. In the case of sterically stabilized liposomes that passively accumulate in solid vascularized tumors *in vivo*, their reported heterogeneous distribution close to perivascular regions and limited movement across the tumor interstitium and mass[19,20,60] limit their therapeutic potential. Recent reports have indicated that improvements in the intratumoral distribution can be achieved in the case of conjugating monoclonal antibody fragments targeting against the herceptin (anti-HER2) receptor, leading to improved therapeutic effects.[61] The interaction of such immunoliposomes with a variety of avascular tumor spheroids will be extremely interesting toward evaluation of their capability to treat metastatic lesions and systematically draw liposome structure (spheroid binding, affinity and diffusion functions) similarly to the present study. Moreover, such work is also of value in the eventual use of liposomes as delivery vehicles for therapeutic radionuclides.[62,63]

This is the first systematic study on the ability of liposomal delivery systems to passively target and diffuse within multicellular tumor spheroids. Taking into account the inherent limitations and restrictions of the tumor spheroid model compared to an *in vivo* or clinical situation, as well as the limitations of the present investigations posed by use of spheroids from a single (LNCaP-LN3) cell line, valuable insight can be obtained on the interaction of delivery systems with 3-dimensional avascular tumor tissue.

TABLE II – QUANTITATIVE EXPRESSION OF BINDING ONTO THE SPHEROIDS, OVERALL AFFINITY FOR THE SPHEROIDS AND THE EXTENT OF LIPOSOME DIFFUSION WITHIN THE TUMOR SPHEROIDS FOLLOWING IMAGE ANALYSIS

Liposome system	Binding[1] (%)	Affinity[2] (a.u.)	Diffusion[3] (%)	
			50 μm (from rim)	100 μm (from rim)
MLV (DMPC:DC-chol)	73.3	7.27	12.3	2.8
MLV (DMPC:DOPE:DC-chol)	60.0	18.3	23.3	4.7
MLV (DMPC:DOPE:DOTAP)	50.2	48.0	29.4	3.8
SUV (DMPC:chol)	38.3	7.3	71.0	49.2
SUV (DMPC:DC-chol)	84.7	3.1	3.4	0.7
SUV (DMPC:DOPE:DC-chol)	76.5	10.3	4.4	2.3
SUV (DMPC:DOPE:DOTAP)	35.6	31.9	62.0	21.4

[1]Fluorescence intensity up to 20 μm deep within the spheroid as a percentage of the total fluorescence intensity signal.–[2]Total fluorescence intensity signal in arbitrary units. –[3]Fluorescence intensity at a particular depth as a percentage of the peak fluorescence intensity.

More work is required employing spheroids from various tumor cell lines to determine the generality of the liposome-spheroid interactions observed here. This is essential towards rational engineering of delivery systems and optimization in the design of *in vivo* experimentation and clinical assessment of any cancer therapeutic modality under development. Particularly relevant toward the clinic, this study indicates some of the critical parameters to engineer efficiently diffusive liposomes able to carry therapeutic agents against avascular micrometastases (such as early-stage prostate or ovarian metastases residing in the peritoneal cavity or in circulation) and solid tumors, able to distribute as homogeneously and deeply toward their hypoxic core following extravasation from the vasculature.

Engineered cationic liposomes with a relatively low charge molar ratio and enhanced fusogenicity, or electrostatically neutral liposomes with fluid bilayers, were found to offer improved distribution characteristics within prostate tumor spheroids. The use of 3-dimensional tumor spheroids and their interaction with liposomes and other delivery systems can provide valuable information and should be more widely used as a tool between the traditional planar cell studies and the *in vivo* and clinical assessment of the delivered culture therapeutics.

REFERENCES

1. Allen TM. Ligand-targeted therapeutics in anticancer therapy. Nat Rev Cancer 2002;2:750–63.
2. Pagnan G, Montaldo PG, Pastorino F, Raffaghello L, Kirchmeier M, Allen TM, Ponzoni M. GD2-mediated melanoma cell targeting and cytotoxicity of liposome-entrapped fenretinide. Int J Cancer 1999;81:268–74.
3. Sapra P, Allen TM. Internalizing antibodies are necessary for improved therapeutic efficacy of antibody-targeted liposomal drugs. Cancer Res 2002;62:7190–4.
4. Xu L, Huang CC, Huang W, Tang WH, Rait A, Yin YZ, Cruz I, Xiang LM, Pirollo KF, Chang EH. Systemic tumor-targeted gene delivery by anti-transferrin receptor scFv-immunoliposomes. Mol Cancer Ther 2002;1:337–46.
5. Pastorino F, Brignole C, Marimpietri D, Sapra P, Moase EH, Allen TM, Ponzoni M. Doxorubicin-loaded Fab′ fragments of anti-disialoganglioside immunoliposomes selectively inhibit the growth and dissemination of human neuroblastoma in nude mice. Cancer Res 2003;63:86–92.
6. Pan XQ, Zheng X, Shi G, Wang H, Ratnam M, Lee RJ. Strategy for the treatment of acute myelogenous leukemia based on folate receptor beta-targeted liposomal doxorubicin combined with receptor induction using all-trans retinoic acid. Blood 2002;100:594–602.
7. Iinuma H, Maruyama K, Okinaga K, Sasaki K, Sekine T, Ishida O, Ogiwara N, Johkura K, Yonemura Y. Intracellular targeting therapy of cisplatin-encapsulated transferrin-polyethylene glycol liposome on peritoneal dissemination of gastric cancer. Int J Cancer 2002;99:130–7.
8. Gijsens A, Derycke A, Missiaen L, De Vos D, Huwyler J, Eberle A, de Witte P. Targeting of the photocytotoxic compound AlPcS4 to Hela cells by transferrin conjugated PEG-liposomes. Int J Cancer 2002;101:78–85.
9. Hood JD, Bednarski M, Frausto R, Guccione S, Reisfeld RA, Xiang R, Cheresh DA. Tumor regression by targeted gene delivery to the neovasculature. Science 2002;296:2404–7.
10. Medina OP, Soderlund T, Laakkonen LJ, Tuominen EK, Koivunen E, Kinnunen PK. Binding of novel peptide inhibitors of type IV collagenases to phospholipid membranes and use in liposome targeting to tumor cells *in vitro*. Cancer Res 2001;61:3978–85.
11. Sihorkar V, Vyas SP. Potential of polysaccharide anchored liposomes in drug delivery, targeting and immunization. J Pharm Pharm Sci 2001;4:138–58.
12. Allen TM, Chonn A. Large unilamellar liposomes with low uptake into the reticuloendothelial system. FEBS Lett 1987;223:42–6.
13. Boman NL, Masin D, Mayer LD, Cullis PR, Bally MB. Liposomal vincristine which exhibits increased drug retention and increased circulation longevity cures mice bearing P388 tumors. Cancer Res 1994;54:2830–3.
14. Woodle MC. Controlling liposome blood clearance by surface-grafted polymers. Adv Drug Deliv Rev 1998;32:139–52.
15. Gabizon A, Catane R, Uziely B, Kaufman B, Safra T, Cohen R, Martin F, Huang A, Barenholz Y. Prolonged circulation time and enhanced accumulation in malignant exudates of doxorubicin encapsulated in polyethylene-glycol coated liposomes. Cancer Res 1994;54:987–92.
16. Klibanov AL, Maruyama K, Torchilin VP, Huang L. Amphipathic polyethyleneglycols effectively prolong the circulation time of liposomes. FEBS Lett 1990;268:235–7.
17. Vaage J, Donovan D, Mayhew E, Uster P, Woodle M. Therapy of mouse mammary carcinomas with vincristine and doxorubicin encapsulated in sterically stabilized liposomes. Int J Cancer 1993;54:959–64.
18. Wu NZ, Braun RD, Gaber MH, Lin GM, Ong ET, Shan S, Papahadjopoulos D, Dewhirst MW. Simultaneous measurement of liposome extravasation and content release in tumors. Microcirculation 1997;4:83–101.
19. Yuan F, Leunig M, Huang SK, Berk DA, Papahadjopoulos D, Jain RK. Microvascular permeability and interstitial penetration of sterically stabilized (stealth) liposomes in a human tumor xenograft. Cancer Res 1994;54:3352–6.
20. Huang SK, Lee KD, Hong K, Friend DS, Papahadjopoulos D. Microscopic localization of sterically stabilized liposomes in colon carcinoma-bearing mice. Cancer Res 1992;52:5135–43.
21. Wu NZ, Da D, Rudoll TL, Needham D, Whorton AR, Dewhirst MW. Increased microvascular permeability contributes to preferential accumulation of stealth liposomes in tumor tissue. Cancer Res 1993;53:3765–70.
22. Sutherland RM. Cell and environment interactions in tumor microregions: the multicell spheroid model. Science 1988;240:177–84.
23. Freyer JP, Sutherland RM. Selective dissociation and characterization of cells from different regions of multicell tumor spheroids. Cancer Res 1980;40:3956–65.
24. Nederman T, Norling B, Glimelius B, Carlsson J, Brunk U. Demonstration of an extracellular matrix in multicellular tumor spheroids. Cancer Res 1984;44:3090–7.
25. Davies Cde L, Berk DA, Pluen A, Jain RK. Comparison of IgG diffusion and extracellular matrix composition in rhabdomyosarcomas

grown in mice *versus in vitro* as spheroids reveals the role of host stromal cells. Br J Cancer 2002;86:1639–44.
26. Helmlinger G, Netti PA, Lichtenbeld HC, Melder RJ, Jain RK. Solid stress inhibits the growth of multicellular tumor spheroids. Nat Biotechnol 1997;15:778–83.
27. Gorlach A, Acker H. pO₂- and pH-gradients in multicellular spheroids and their relationship to cellular metabolism and radiation sensitivity of malignant human tumor cells. Biochim Biophys Acta 1994;1227:105–12.
28. Waleh NS, Brody MD, Knapp MA, Mendonca HL, Lord EM, Koch CJ, Laderoute KR, Sutherland RM. Mapping of the vascular endothelial growth factor-producing hypoxic cells in multicellular tumor spheroids using a hypoxia-specific marker. Cancer Res 1995;55:6222–6.
29. Gilead A, Meir G, Neeman M. The role of angiogenesis, vascular maturation, regression and stroma infiltration in dormancy and growth of implanted MLS ovarian carcinoma spheroids. Int J Cancer 2004;108:524–31.
30. Sarfaraz M, Wessels BW. Validation of an analytical expression for the absorbed dose from a spherical beta source geometry and its application to micrometastatic radionuclide therapy. Clin Cancer Res 1999;5(Suppl 10):3020S–23S.
31. Walker KA, Mairs R, Murray T, Hilditch TE, Wheldon TE, Gregor A, Hann IM. Tumor spheroid model for the biologically targeted radiotherapy of neuroblastoma micrometastases. Cancer Res 1990;50(Suppl 3):1000S–2S.
32. Ballangrud AM, Yang WH, Charlton DE, McDevitt MR, Hamacher KA, Panageas KS, Ma D, Bander NH, Scheinberg DA, Sgouros G. Response of LNCaP spheroids after treatment with an alpha-particle emitter (213Bi)-labeled anti-prostate-specific membrane antigen antibody (J591). Cancer Res 2001;61:2008–14.
33. Boucher Y, Leunig M, Jain RK. Tumor angiogenesis and interstitial hypertension. Cancer Res 1996;56:4264–6.
34. Paulus W, Huettner C, Tonn JC. Collagens, integrins and the mesenchymal drift in glioblastomas: a comparison of biopsy specimens, spheroid and early monolayer cultures. Int J Cancer 1994;58:841–6.
35. Campbell RB, Fukumura D, Brown EB, Mazzola LM, Izumi Y, Jain RK, Torchilin VP, Munn LL. Cationic charge determines the distribution of liposomes between the vascular and extravascular compartments of tumors. Cancer Res 2002;62:6831–6.
36. Ballangrud AM, Yang WH, Dnistrian A, Lampen NM, Sgouros G. Growth and characterization of LNCaP prostate cancer cell spheroids. Clin Cancer Res 1999;5(Suppl 10):3171S–6S.
37. Litzinger DC, Buiting AM, van Rooijen N, Huang L. Effect of liposome size on the circulation time and intraorgan distribution of amphipathic poly(ethylene glycol)-containing liposomes. Biochim Biophys Acta 1994;1190:99–107.
38. Claassen E. Post-formation fluorescent labelling of liposomal membranes: *in vivo* detection, localisation and kinetics. J Immunol Methods 1992;147:231–40.
39. McLean JW, Fox EA, Baluk P, Bolton PB, Haskell A, Pearlman R, Thurston G, Umemoto EY, McDonald DM. Organ-specific endothelial cell uptake of cationic liposome-DNA complexes in mice. Am J Physiol 1997;273(1 Pt 2):H387–404.
40. Mui BL, Cullis PR, Evans EA, Madden TD. Osmotic properties of large unilamellar vesicles prepared by extrusion. Biophys J 1993;64:443–53.
41. Yuhas JM, Li AP, Martinez AO, Ladman AJ. A simplified method for production and growth of multicellular tumor spheroids. Cancer Res 1977;37:3639–43.
42. Hafez IM, Cullis PR. Roles of lipid polymorphism in intracellular delivery. Adv Drug Deliv Rev 2001;47:139–48.
43. Parthasarathy R, Sacks PG, Harris D, Brock H, Mehta K. Interaction of liposome-associated all-trans-retinoic acid with squamous carcinoma cells. Cancer Chemother Pharmacol 1994;34:527–34.
44. Sacks PG, Oke V, Mehta K. Antiproliferative effects of free and liposome-encapsulated retinoic acid in a squamous carcinoma model: monolayer cells and multicellular tumor spheroids. J Cancer Res Clin Oncol 1992;118:490–6.
45. Weber F, Kremer C, Klinkhammer M, Rasier B, Brock M. Response of multicellular tumor spheroids to liposomes containing TNF-alpha. J Neurooncol 1994;18:217–24.
46. Tsukioka YMY, Hamaguchi T, Koike H, Moriyasu F, Kakizoe T. Pharmaceutical and biomedical differences between micellar doxorubicin (NK911) and liposomal doxorubicin (Doxil). Jpn J Cancer Res 2002;93:1145–53.
47. Pluen A, Boucher Y, Ramanujan S. Role of tumor-host interactions in interstitial diffusion of macromolecules: cranial *vs.* subcutaneous tumors. Proc Natl Acad Sci USA 2001;98:4628–33.
48. Adlakha-Hutcheon G, Bally MB, Shew CR, Madden TD. Controlled destabilization of a liposomal drug delivery system enhances mitoxantrone antitumor activity. Nat Biotechnol 1999;17:775–9.
49. Walker KA, Murray T, Hilditch TE, Wheldon TE, Gregor A, Hann IM. A tumour spheroid model for antibody-targeted therapy of micrometastases. Br J Cancer 1988;58:13–6.
50. Cheng FM, Hansen EB, Taylor CR, Epstein AL. Diffusion and binding of monoclonal antibody TNT-1 in multicellular tumor spheroids. J Natl Cancer Inst 1991;83:200–4.
51. Hjelstuen MH, Rasch-Halvorsen K, Bruland O, De LDC. Uptake, penetration, and binding of monoclonal antibodies with increasing affinity in human osteosarcoma multicell spheroids. Anticancer Res 1998;18:3153–61.
52. Koike C, McKee TD, Pluen A, Ramanujan S, Burton K, Munn LL, Boucher Y, Jain RK. Solid stress facilitates spheroid formation: potential involvement of hyaluronan. Br J Cancer 2002;86:947–53.
53. Felgner PL, Tsai YJ, Sukhu L, Wheeler CJ, Manthorpe M, Marshall J, Cheng SH. Improved cationic lipid formulations for *in vivo* gene therapy. Ann NY Acad Sci 1995;772:126–39.
54. Thurston G, McLean JW, Rizen M, Baluk P, Haskell A, Murphy TJ, Hanahan D, McDonald DM. Cationic liposomes target angiogenic endothelial cells in tumors and chronic inflammation in mice. J Clin Invest 1998;101:1401–13.
55. Krasnici S, Werner A, Eichhorn ME, Schmitt-Sody M, Pahernik SA, Sauer B, Schulze B, Teifel M, Michaelis U, Naujoks K, Dellian M. Effect of the surface charge of liposomes on their uptake by angiogenic tumor vessels. Int J Cancer 2003;105:561–7.
56. Saga T, Neumann RD, Heya T, Sato J, Kinuya S, Le N, Paik CH, Weinstein JN. Targeting cancer micrometastases with monoclonal antibodies: a binding-site barrier. Proc Natl Acad Sci USA 1995;92:8999–9003.
57. Jain RK. Delivery of molecular and cellular medicine to solid tumors. Adv Drug Deliv Rev 2001;46:149–68.
58. Graff CP, Wittrup KD. Theoretical analysis of antibody targeting of tumor spheroids: importance of dosage for penetration, and affinity for retention. Cancer Res 2003;63:1288–96.
59. Juweid M, Neumann R, Paik C, Perez-Bacete MJ, Sato J, van Osdol W, Weinstein JN. Micropharmacology of monoclonal antibodies in solid tumors: direct experimental evidence for a binding site barrier. Cancer Res 1992;52:5144–53.
60. Ishida O, Maruyama K, Sasaki K, Iwatsuru M. Size-dependent extravasation and interstitial localization of polyethyleneglycol liposomes in solid tumor-bearing mice. Int J Pharm 1999;190:49–56.
61. Park JW, Hong K, Kirpotin DB, Colbern G, Shalaby R, Baselga J, Shao Y, Nielsen UB, Marks JD, Moore D, Papahadjopoulos D, Benz CC. Anti-HER2 immunoliposomes: enhanced efficacy attributable to targeted delivery. Clin Cancer Res 2002;8:1172–81.
62. Emfietzoglou D, Kostarelos K, Sgouros G. An analytic dosimetry study for the use of radionuclide-liposome conjugates in internal radiotherapy. J Nucl Med 2001;42:499–504.
63. Sofou STJ, Lin H, Pellegrini V, Palm S, McDevitt MR, Scheinberg DA, Sgouros G. Vesicular nanocarriers for targeted alpha-particle therapy of metastatic cancer. Cancer Biother Radiopharm 2002;17:476.